JOURNAL OF MATERIALS SCIENCE 18 (1983) 2337–2344

The hydrostatic pressure derivatives of the elastic constants of bismuth alloys

TU. HAILING, G. A. SAUNDERS
School of Physics, University of Bath, Claverton Down, Bath, UK

Measurements of the effect of hydrostatic pressure on the velocity of ultrasonic waves have been used to obtain the pressure derivatives ($\partial C_{IJ}/\partial P$) of the elastic constants of single crystals of a bismuth–10 at % antimony alloy and of heavily tellurium-doped (n-type) bismuth. A theoretical model is used to predict that there should be no electronic (L to L point) contributions to these pressure derivatives. This is established experimentally by the finding that the $\partial C_{IJ}/\partial P$ values of the n-type bismuth doped with tellurium (carrier density $n = 1.2 \times 10^{20}$ cm^{-3}) are the same within experimental error as those of pure bismuth. The zone centre acoustic mode Grüneisen parameters, obtained from the elastic constants and their pressure derivatives, are used to quantify the anharmonicity of the acoustic mode lattice vibrations for these bismuth alloys. It is concluded that the vibrational anharmonicity of bismuth is insensitive to alloying with up to 10 at % antimony.

1. Introduction

Over a wide range of concentration (~ 7 to ~ 40 at % antimony), the bismuth–antimony alloys are narrow gap semiconductors, and their device potential has led to extensive studies of their electronic properties. The elastic stiffness constants of selected alloy compositions have also been measured [1]. However, no information is available on the effects of hydrostatic pressure on the lattice dynamical behaviour of these alloys. In this paper ultrasonic measurements of the elastic constants under pressure of a semiconducting bismuth–antimony alloy are reported. The elastic constants themselves are a measure of the slopes of the acoustic branch of phonon dispersion curves at the Brillouin zone centre, while the pressure derivatives of the elastic constants determine the change of these slopes with pressure. Thus the pressure derivatives of the elastic constants provide information about the vibrational anharmonicity, that is the nonlinearity of interatomic forces with respect to atomic displacements. At high temperatures all physical properties which depend upon thermal motion are influenced by anharmonicity so that its knowledge is fundamental to an understanding of material properties such as thermal expansion, crystal stability and mechanical strength. The usual practice is to discuss anharmonicity in terms of a Grüneisen parameter and the gammas appropriate to the zone centre acoustic modes are presented here. The temperature dependences of the elastic constants of bismuth and its alloys with up to 10 at % antimony have been found previously to be very similar, suggesting that the lattice anharmonicity of bismuth is not sensitive to alloying with its neighbouring group V element antimony. The pressure dependences of the elastic constants enable this suggestion to be examined quantitatively.

There can be measurable electronic contributions to the elastic constants of a many valleyed semi-metal, like bismuth, or semiconductor, such as the bismuth–antimony alloys. A theoretical study has been undertaken to assess whether any electronic contributions to the hydrostatic pressure derivatives of the elastic constants are to be expected. Testing of the predictions of this theory is simpler using heavily n-type doped bismuth than with the bismuth–antimony alloys themselves. Hence the hydrostatic pressure derivatives of the elastic constants of a tellurium-doped

0022–2461/83 $03.00 + .12

bismuth crystal have been measured and these are also reported here.

2. Experimental procedure and results

The single crystals of bismuth–10 at% antimony and tellurium-doped bismuth were grown by the repeated pass, zone melting technique. The elastic constants of the bismuth–antimony alloy crystals formed part of a wider study of ultrasonic wave velocities in a number of alloys in the series by Lichnowski and Saunders [1], whose paper gives further details of crystal growth and ultrasonic sample preparation. The single crystals of the tellurium-doped bismuth were those (denoted T20) used by Lichnowski and Saunders [2] to determine the electronic contributions to the elastic constants of bismuth. Tellurium acts as an electron donor in bismuth; the carrier concentration determined by galvanomagnetic measurements at room temperature in this n-type material is $1.2 \times 10^{20}\,\mathrm{cm}^{-3}$. Radioactive tracer experiments have shown that tellurium is a monovalent donor in bismuth [3]. Hence it can be assumed that each tellurium atom contributes one electron to the L-point ellipsoids. To give an electron concentration of $1.2 \times 10^{20}\,\mathrm{cm}^{-3}$ requires a tellurium concentration in the alloy 0.43 at%.

The crystals were orientated by the Laue back reflection technique, and faces, perpendicular to the crystallographic direction in which the ultrasonic waves were to be propagated, were cut and polished parallel to better than 10^{-4} rad. Ultrasonic wave transit times were measured by the single ended pulse echo technique to 1 part in 10^5. The second order elastic constants of the 10 at% antimony alloy have been reported between 4.2 and 300 K by Lichnowski and Saunders [1] and of the tellurium-doped bismuth crystal (T20) also by Lichnowski and Saunders [2].

Hydrostatic pressure measurements were made in a piston-and-cylinder apparatus, the pressure being determined by means of a pre-calibrated manganin resistance coil. Further details of the apparatus and techniques employed can be found elsewhere [4].

To avoid the need to calculate changes in crystal dimensions under pressure, the "natural" velocity W technique [5] has been used. Hence experimental measurements of the change in pulse echo overlap frequency induce by application of hydrostatic pressure have been converted to relative change, $\Delta W/W_0$, of natural velocity. Results for a number of ultrasonic modes in the bismuth–10 at% antimony alloy are shown in Fig. 1, and those for the tellurium-doped bismuth in Fig. 2. The effect of pressure on the ultrasonic wave velocity can be seen to be linear over the pressure range examined.

The initial pressure derivative $(\rho V^2)'_{P=0}$ is given by [6]

$$(\rho V^2)'_{P=0} = \rho V_0^2(2f'/f_0 + \beta^T - 2N_k N_m S^T_{kmii})_{P=0} \tag{1}$$

where V_0 is the mode velocity at atmospheric pressure, f is the pulse echo overlap frequency at atmospheric pressure and f' is its pressure derivative. For $\bar{3}m$ Laue group rhombohedral crystals, these equations reduce to the following expressions for the effective pressure derivatives $\partial C_{IJ}/\partial P$:

$$\begin{aligned}
\frac{\partial C_{11}}{\partial P} &= C_{11}\left(\frac{2f'}{f} + 2S_{13} + S_{33}\right)\\
\frac{\partial C_{66}}{\partial P} &= C_{66}\left(\frac{2f'}{f} + 2S_{13} + S_{33}\right)\\
\frac{\partial C_{33}}{\partial P} &= C_{33}\left(\frac{2f'}{f} + 2S_{11} + 2S_{12} - S_{33}\right)\\
\frac{\partial C_{44}}{\partial P} &= C_{44}\left(\frac{2f'}{f} + 2S_{11} + 2S_{12} - S_{33}\right)\\
\frac{\partial C'}{\partial P} &= C'\left(\frac{2f'}{f} + S_{11} + S_{12} + S_{13}\right)\\
\frac{\partial C''}{\partial P} &= C''\left(\frac{2f'}{f} + 2S_{13} + S_{33}\right)
\end{aligned} \tag{2}$$

where

$$\begin{aligned}
C' &= \tfrac{1}{2}\{\tfrac{1}{2}(C_{11} + C_{33}) + C_{44} - C_{14}\\
&\quad - [(\tfrac{1}{2}C_{11} - \tfrac{1}{2}C_{33} - C_{14})^2\\
&\quad + (C_{13} + C_{44} - C_{14})^2]^{1/2}\}\\
C'' &= \tfrac{1}{2}\{(C_{66} + C_{44}) + [(C_{44} - C_{66})^2 + 4C_{14}^2]^{1/2}\}
\end{aligned} \tag{3}$$

Here the isothermal compressibility β^T $(= \beta^S + T\beta^2/\rho C_p)$ has been replaced by the adiabatic compressibility β^S due to the lack of extensive thermodynamic data for the alloys; however the error introduced can only be of the order of 1%. The pressure derivatives $\partial C_{IJ}/\partial P$ for the bismuth–10 at% antimony alloy and the tellurium-doped bismuth crystal are compared with those of pure bismuth in Table I. A second way of expressing the data is in the form of thermodynamic coef-

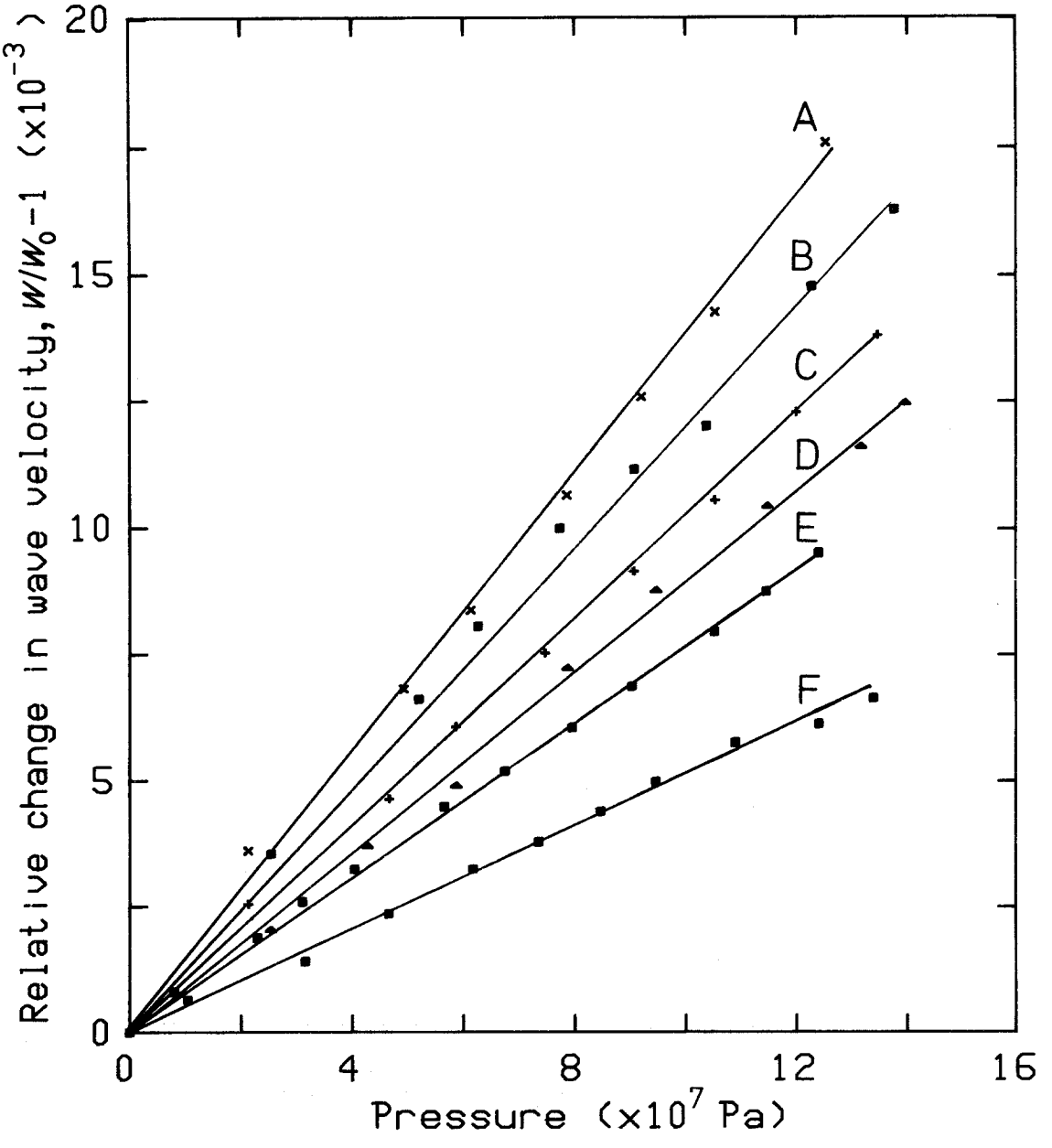

Figure 1 Relative change in natural wave velocity in bismuth–10 at % antimony alloy crystals under hydrostatic pressure. The modes are: A: N[0 0 1], U[1 0 0]; B: N[0 $-\frac{1}{\sqrt{2}}$ $\frac{1}{\sqrt{2}}$], U[0 $-\frac{1}{\sqrt{2}}$ $\frac{1}{\sqrt{2}}$]; C: N[0 0 1], U[0 0 1]: D: N[1 0 0], U[0 1 0]; E: N[0 0 1], U[0 1 0]; F: N[1 0 0], U[1 0 0].

ficients, which are defined in terms of the second derivatives with respect to strain of the initial energy [6]. For a $\bar{3}m$ Laue group rhombohedral crystal, it can be shown that the hydrostatic pressure derivatives of the thermodynamic second order stiffness are related to the $\partial C_{IJ}/\partial P$ by

$$B_{11} = \partial C_{11}/\partial P + 1 - (S_3 - 2S_1)C_{11}$$
$$B_{66} = \partial C_{66}/\partial P + 1 - (S_3 - 2S_1)C_{66}$$
$$B_{33} = \partial C_{33}/\partial P + 1 - (2S_1 - 3S_3)C_{33}$$
$$B_{44} = \partial C_{44}/\partial P + 1 + S_3 C_{44}$$
$$B_{13} = \partial C_{13}/\partial P - 1 + S_3 C_{13}$$
$$B_{14} = \partial C_{14}/\partial P + S_1 C_{14} \quad (4)$$

where $S_1 = S_2 = S_{11} + S_{12} + S_{13}$ and $S_3 = 2S_{13} + S_{33}$. These pressure derivatives B_{IJ}, also given in Table I, are useful in calculating the mode Grüneisen parameters.

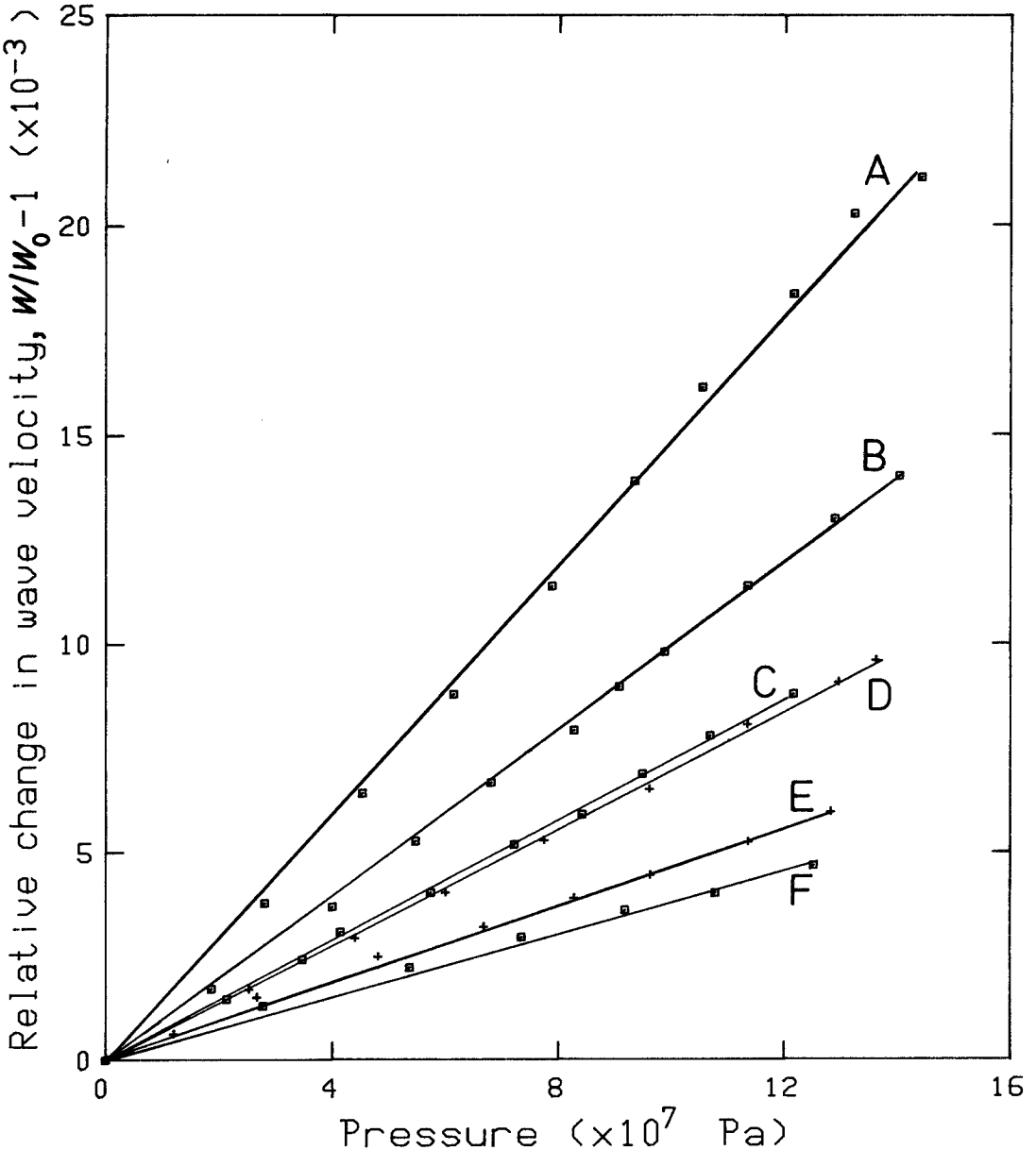

Figure 2 Relative change in natural wave velocity in tellurium-doped bismuth crystals (T20) under hydrostatic pressure. The modes are: A: N[0 $\frac{1}{\sqrt{2}}$ $\frac{1}{\sqrt{2}}$], U[0 $\frac{1}{\sqrt{2}}$ $\frac{1}{\sqrt{2}}$]; B: N[0 0 1], U[0 0 1]; C: N[0 0 1], U[1 0 0]; D: N[1 0 0], U[1 0 0]; E: N[1 0 0], U[0 1 0]; F: N[0 $\frac{1}{\sqrt{2}}$ $\frac{1}{\sqrt{2}}$], U[0 $-\frac{1}{\sqrt{2}}$ $\frac{1}{\sqrt{2}}$].

3. Discussion

The free energy in semi-metals and semiconductors includes a free carrier contribution. In a many valleyed material, application of a strain can induce a shift of the band extrema relative to each other, the free carriers redistribute to minimize the free energy, and the effective elastic stiffness is reduced [7, 8]. The electron Fermi surface of bismuth consists of three geometrically equivalent prolate ellipsoids each centred about energy minima at the L points on the six irregular hexagon faces of the Brillouin zone (for a detailed description see the review [9]). At the L point there is a valence band separated from the conduction band by a small energy gap E_g (13.6 eV) [10]; interaction between this and the conduction band results in a non-parabolic dependence of momentum upon energy. Lichnowski and Saunders [2] have extended the Keyes' model to show that the electronic (L to L point) contri-

TABLE I The effective pressure derivatives $\partial C_{IJ}/\partial P$ and the pressure derivatives B_{IJ} of the thermodynamic second order elastic constants at 290 K for bismuth–10 at % antimony and bismuth–0.43 at % tellurium compared with the data for pure bismuth. The units of the second order elastic constants C_{IJ} are 10^9 N m^{-2}

	Bi–10 at % Sb	Bi–0.43 at % Te	Bi [1, 13]	Errors
$\partial C_{11}/\partial P$	6.9	6.7	6.38	± 3%
$\partial C_{12}/\partial P$	3.7	3.6	2.38	± 20%
$\partial C_{13}/\partial P$	4.4	4.8	4.69	± 10%
$\partial C_{14}/\partial P$	2.0	2.0	1.70	± 10%
$\partial C_{33}/\partial P$	7.4	7.4	6.62	± 5%
$\partial C_{44}/\partial P$	3.6	3.4	3.37	± 1%
$\partial C_{66}/\partial P$	1.6	1.6	2.00	± 12%
B_{11}	8.1	7.5	6.98	
B_{12}	2.7	2.5	1.44	
B_{13}	3.0	3.3	4.14	
B_{14}	2.0	2.1	1.84	
B_{33}	9.8	10.0	9.20	
B_{44}	4.8	4.6	4.58	
B_{66}	2.5	2.5	2.80	
C_{11}	66.8	61.4	63.4	
C_{12}	24.4	25.5	24.5	
C_{13}	24.7	24.3	24.9	
C_{14}	8.3	7.42	7.28	
C_{33}	37.9	37.7	37.9	
C_{44}	13.1	11.6	11.5	
C_{66}	21.2	18.0	19.4	

butions to the second order elastic constants of bismuth in the non-ellipsoidal, non-parabolic band (NENP) model are given by

$$\begin{aligned}
\Delta C_{11} &= -(9/2)(L_{11}-L_{22})^2\gamma \\
\Delta C_{12} &= +(9/2)(L_{11}-L_{22})^2\gamma \\
\Delta C_{14} &= -9(L_{11}-L_{22})L_{23}\gamma \\
\Delta C_{44} &= -18L_{23}^2\gamma \\
\Delta C_{13} &= \Delta C_{33} = 0 \\
\Delta C_{66} &= \Delta C_{11} = -\Delta C_{12}
\end{aligned} \tag{5}$$

where

$$\gamma = \frac{\pi^{-1/2}}{12} N_c (kT)^{-1} [F_{-1/2}(\eta) + (6kT/E_g)F_{1/2}(\eta)] \tag{6}$$

and

$$N_c = 2(2\pi m_e^* kT/h^2)^{3/2} \tag{7}$$

The L_{ij} are components of the deformation potential tensor, $F_{-1/2}(\eta)$, and $F_{1/2}(\eta)$ are Fermi–Dirac integrals in the reduced Fermi energy $\eta(= E_{F_0}^e/kT)$ and $m_e^*(= m_1^* m_2^* m_3^*)^{1/3}$ is the band edge, density of states effective mass. Donor-doping of bismuth with tellurium produces changes in the elastic constants which are consistent with these predicted L to L point contributions [2].

It is useful to know whether the L to L point carrier redistributions can influence the hydrostatic pressure derivatives $\partial C_{IJ}/\partial P$ of the elastic constants, as such an effect might lead to measurable differences between the $\partial C_{IJ}/\partial P$ values for pure bismuth and tellurium-doped bismuth, as it does for the second order elastic constants C_{11}, C_{12}, C_{66} and C_{14} (and in principle for C_{44} as well) [2]. The theoretical situation for the $\partial C_{IJ}/\partial P$ can be worked out by considering the L to L point effects on the third order elastic constants (C_{IJK}) and combining the results with those given in Equation 5 for the second order constants. The influence of the L to L point transitions on the C_{IJK} can be obtained [11] from the cubic term in the electronic free energy

$$\begin{aligned}
F_{el} = {} & \frac{1}{4}\sum_{i=1}^{3}\sum_{j=1}^{3}(W^{(i)}-W^{(j)})^2\phi^{(i)}\phi^{(j)} \Big/ \sum_{i=1}^{3}\phi^{(i)} \\
& + \frac{1}{6}\sum_{i=1}^{3}\sum_{j=1}^{3}\sum_{k=1}^{3}\sum_{l=1}^{3}\Bigg((W^{(i)}-W^{(j)}) \\
& \times (W^{(i)}-W^{(k)})(W^{(i)}-W^{(l)})\phi^{(j)}\phi^{(k)}\phi^{(l)} \\
& \times \int N^{(i)}(E)(\partial^2 f_0/\partial E^2)\,dE\Bigg)\Bigg(\sum\phi^{(i)}\Bigg)^{-3}
\end{aligned} \tag{8}$$

Here $W^{(i)}$ is the strain induced shift in the energy of the ith valley and the effective density of states at the Fermi surface is:

$$\phi^{(i)} = \int_{E^i}^{\infty} N^{(i)}(E)[\partial f(E, E_{F_0}^e)/\partial E]\,dE \tag{9}$$

The L to L point contributions ΔC_{IJK} to the third order elastic constants of bismuth can be shown to be

$$\begin{aligned}
\Delta C_{111} &= \Delta C_{222} = \Delta C_{155} = \Delta C_{112} = \Delta C_{124} \\
&= \tfrac{81}{16}(L_{11}-L_{22})^3\gamma' \\
\Delta C_{114} &= \tfrac{81}{16}L_{23}(L_{11}-L_{22})^2\gamma' \\
\Delta C_{144} &= -\tfrac{81}{8}(L_{11}-L_{22})L_{23}^2\gamma' \\
\Delta C_{444} &= \tfrac{162}{4}L_{23}^3\gamma' \\
\Delta C_{113} &= \Delta C_{123} = \Delta C_{133} = \Delta C_{134} \\
&= \Delta C_{333} = \Delta C_{344} = 0 \qquad (10)
\end{aligned}$$

For a NENP band model γ' is a complex function of second derivatives of the Fermi–Dirac integral.

Now the hydrostatic pressure derivatives $\partial C_{IJ}/\partial P$ of the second order elastic constants for a rhombohedral $\bar{3}m$ Laue group crystal can be shown to be:

$$\begin{aligned}
\frac{\partial C_{11}}{\partial P} &= -\left[1+\frac{2C_{11}C_{33}-C_{11}^2-C_{11}C_{12}+(C_{33}-C_{13})(C_{111}+C_{112})+(C_{11}+C_{12}-2C_{13})C_{113}}{C_{33}(C_{11}+C_{12})-2C_{13}^2}\right] \\
\frac{\partial C_{12}}{\partial P} &= -\left[-1+\frac{2C_{12}C_{33}-C_{11}C_{12}-C_{12}^2+(C_{33}-C_{13})(C_{111}+2C_{112}-C_{222})+(C_{11}+C_{12}-2C_{13})C_{123}}{C_{33}(C_{11}+C_{12})-2C_{13}^2}\right] \\
\frac{\partial C_{13}}{\partial P} &= -\left[-1+\frac{C_{11}C_{13}+C_{12}C_{13}-2C_{13}^2+(C_{33}-C_{13})(C_{113}+C_{123})+(C_{11}+C_{12}-2C_{13})C_{133}}{C_{33}(C_{11}+C_{12})-2C_{13}^2}\right] \\
\frac{\partial C_{14}}{\partial P} &= -\left[\frac{C_{14}C_{33}-C_{13}C_{14}+(C_{33}-C_{13})(C_{114}+C_{124})+(C_{11}+C_{12}-2C_{13})C_{134}}{C_{33}(C_{11}+C_{12})-2C_{13}^2}\right] \\
\frac{\partial C_{33}}{\partial P} &= -\left[1+\frac{3C_{11}C_{33}+3C_{12}C_{33}-4C_{13}C_{33}-2C_{33}^2+2(C_{33}-C_{13})C_{133}+(C_{11}+C_{12}-2C_{13})C_{333}}{C_{33}(C_{11}+C_{12})-2C_{13}^2}\right] \\
\frac{\partial C_{44}}{\partial P} &= -\left[1+\frac{C_{11}C_{44}+C_{12}C_{44}-2C_{13}C_{44}+(C_{33}+C_{13})(C_{144}+C_{155})+(C_{11}+C_{12}-2C_{13})C_{344}}{C_{33}(C_{11}+C_{12})-2C_{13}^2}\right] \\
\frac{\partial C_{66}}{\partial P} &= -\left[1+\frac{2C_{11}C_{33}+C_{12}^2-C_{11}^2-2C_{12}C_{33}+(C_{11}-C_{13})(C_{222}-C_{112})+(C_{11}+C_{12}-2C_{13})(C_{113}-C_{123})}{2C_{33}(C_{11}+C_{12})-4C_{13}^2}\right]
\end{aligned} \qquad (11)$$

Substitution of the Equations 5 and 10 for the electronic contributions ΔC_{IJ} and ΔC_{IJK} into these Equations 11 in the form for $\Delta(\partial C_{IJ}/\partial P)$ shows that all the terms cancel so that each $\Delta(\partial C_{IJ}/\partial P)$ is zero. There are no electronic contributions to the hydrostatic pressure derivatives of the elastic constants, although certain elastic constants themselves do depend upon electron concentration. Hole contributions and electron–hole interactions can also be shown to be absent (both are insignificant in bismuth [2]). For antimony which has a multi-valley hole, Fermi surface some components of C_{IJ} and C_{IJK} can include free carrier contributions. The hydrostatic pressure derivatives $\partial C_{IJ}/\partial P$ of the elastic constants of tellurium-doped bismuth measured here are the same within experimental error as those of pure bismuth (Table I). This is in agreement with the theoretical prediction. The strains induced by certain ultrasonic modes break the symmetry of the crystal and thus of the Fermi surface – this leads to the strain induced band edge shifts and the extra free energy contribution which produces non-zero values of some individual ΔC_{IJ} and ΔC_{IJK} (Equations 5 and 10). However, application of hydrostatic pressure has no further influence on symmetry and hence no effect on the derivatives $\partial C_{IJ}/\partial P$.

These arguments also apply to the bismuth–antimony alloys–there should be little dependence of the derivatives $\partial C_{IJ}/\partial P$ on the doping level.

The measurements of the pressure derivatives of the elastic constants enable a quantitative determination of the vibrational anharmonicity associated with the long wavelength acoustic modes for the bismuth alloys. The usual practice of discussing anharmonic effects in terms of Grüneisen parameters will be followed. The generalized Grüneisen mode gammas specify the isothermal strain dependence of the frequency $\omega_p(\mathbf{q})$ of a lattice mode of wave vector $\mathbf{q}$ and branch $p(=1,2,3)$.

$$_{jk}\gamma_p^T(\mathbf{q}) = -\left\{\frac{1}{\omega_p(\mathbf{q})}\left[\frac{\partial\omega_p(\mathbf{q})}{\partial\eta_{jk}}\right]_T\right\}_{\eta=0} \quad (12)$$

Here η_{jk} are components of the Lagrangian strain tensor. The general relationship expressing the acoustic mode Grüneisen parameter $H\Gamma_p^T(\mathbf{N})$ in terms of second order and third order elastic constants [12] is

$$H\Gamma_p^T(\mathbf{N}) = -[2\beta^T\omega_p(\mathbf{N})]^{-1}\{1 + S_{aajk}^T \times [2\omega_p(\mathbf{N})U_jU_k + C_{jkmunv}N_mN_nU_uU_v]\} \quad (13a)$$

For rhombohedral crystals belonging to the $\bar{3}m$ Laue group, by using the pressure derivatives of the thermodynamic coefficients B_{IJ}, a specialized form has been developed as follows:

$$\begin{aligned} H\Gamma_p^T(\mathbf{N}) = &-(2\omega\beta^T)^{-1} \\ &\times\{1 + 2\omega[S_1(U_1^2+U_2^2) + S_3U_3^2] \\ &- B_{11}(N_1U_1 + N_2U_2)^2 \\ &- B_{66}(N_1N_2 - N_2U_1)^2 \\ &- B_{33}N_3^2U_3^2 - B_{44}[(N_2U_3 \\ &+ N_3U_2)^2 + (N_3U_1 + N_1U_3)^2] \\ &- 2B_{13}(N_1N_3U_1U_3 + N_2N_3U_2U_3) \\ &- 2B_{14}(N_1^2U_2U_3 + 2N_2N_3U_1U_3 \\ &+ 2N_1N_3U_1U_2 - N_2^2U_2U_3 \\ &+ N_2N_3U_1^2 - N_2N_3U_2^2)\} \end{aligned}$$

where

$$\begin{aligned} \omega = &C_{11}(N_1U_1 + N_2U_2)^2 + C_{66}(N_1U_2 \\ &- N_2U_1)^2 + C_{33}N_3^2U_3^2 + C_{44}[(N_2U_3 \\ &+ N_3U_2)^2 + (N_3U_1 + N_1U_3)^2] \\ &+ 2C_{13}(N_1N_3U_1U_3 + N_2N_3U_2U_3) \\ &+ 2C_{14}(N_1^2U_2U_3 + 2N_1N_2U_1U_3 \\ &+ 2N_1N_3U_1U_2 - N_2^2U_2U_3 \\ &+ N_2N_3U_1^2 - N_2N_3U_2^2) \end{aligned} \quad (13b)$$

The acoustic mode Grüneisen gammas have been computed as a function of orientation using as input data the second order elastic constant and pressure derivative data given in Table I. Results are plotted for the bismuth–antimony alloy in Fig. 3 and for the heavily tellurium-doped bismuth in Fig. 4. These parameters are similar to those of bismuth itself [13]. In the absence of a lattice instability in the form of mode softening, it is usual that the elastic constants and the lattice vibrational frequencies increase under pressure; the Grüneisen parameters should then be positive. Since this is so for all acoustic modes propagated in any direction, there is no evidence for mode softening in the alloys which show normal behaviour of the zone centre acoustic mode frequencies under pressure. The group V semi-

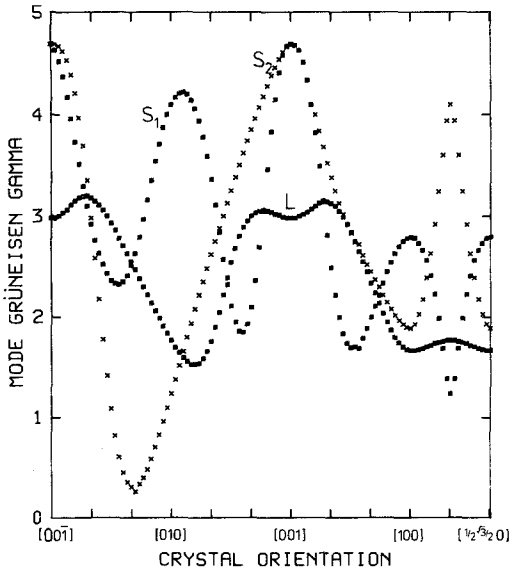

Figure 3 The zone centre, acoustic mode Grüneisen parameters of bismuth–10 at % antimony alloy as a function of mode propagation direction.

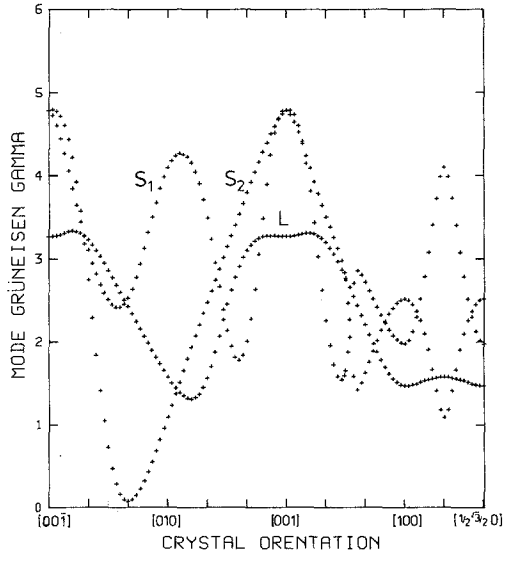

Figure 4 The zone centre, acoustic mode Grüneisen parameters of bismuth doped with tellurium (T20) as a function of mode propagation direction.

metals show a tendency towards behaving as layer-like materials with tighter interatomic binding within a double-layered plane than in the direction (z) normal to the layers [14].

The ease of cleavage to expose xy planes illustrates this property. The application of hydrostatic pressure to a uniaxial crystal can produce a quite different contraction along the major symmetry axis than in the plane normal to it. For layer-like crystals such as the group V semi-metals, the linear compressibility β_l ($= S_{ijkk} m_i m_j$ in the direction of a unit vector **m**) is much larger in the direction perpendicular to the layer planes than in the plane normal [14]. In a rhombohedral crystal the linear compressibility has two components:

$$\beta_z = 2S_{13} + S_{33} \quad (14)$$

and the other normal to this trigonal direction:

$$\beta_{xy} = S_{11} + S_{12} + S_{13} \quad (15)$$

For pure bismuth β_z is $18.1 \times 10^{-12} \mathrm{m^2 N^{-1}}$ while β_{xy} is $6.4 \times 10^{-12} \mathrm{m^2 N^{-1}}$, for the tellurium-doped crystal these compressibilities are 18.3 and 6.4 respectively and for the bismuth–antimony alloy 18.7 and 5.9 (in the same units), respectively. Thus the alloys show the same anisotropy of compressibility as the pure element, which points to closely similar interatomic binding forces in the double layer model. The anisotropy of the mode Grüneisen parameters (Fig. 3) concurs with this double layer model for the bismuth–antimony alloy. Since the major effect of hydrostatic pressure is to squeeze the layers together ($\beta_z > \beta_{xy}$), the effect of the repulsive forces between the double layers must be particularly important for modes propagated down the z-axis. Hence the Grüneisen parameter for z-axis modes tends to be large (Fig. 3).

The temperature dependences of the ultrasonic wave velocities in bismuth–antimony crystals are almost unaltered by alloying [1]. Now an elastic constant $C_{IJ}(T)$ at a temperature T can be written [1, 15] as

$$C_{IJ}(T) = C_{IJ}(0)[1 - K_{IJ} F(T/\theta_D)] \quad (16)$$

where $C_{IJ}(0)$ is that at $T = 0\,\mathrm{K}$. K_{IJ} is a constant which depends upon the anharmoncity of the lattice vibrations and can be expressed empirically as

$$K_{IJ} = 9\beta_\infty \theta_D L(C_1/C) \quad (17)$$

where C_1/C is an anharmonic to harmonic force constant ratio and β_∞ is the thermal expansion at infinite temperature. Thus the physical source of the temperature dependences of an elastic constant, expressed approximately by Equation 16, lies in the anharmonicity of the lattice vibrations. Therefore, the lack of compositional dependence of the temperature dependence of the elastic constants suggests that the anharmonicity of bismuth is not sensitive to alloying with up to 10 at% antimony [1]. The close similarity between the hydrostatic pressure of the elastic constants of bismuth and those of the bismuth–antimony alloy (Table I) confirm this suggestion.

Acknowledgement

We are most grateful to J. Penfold and Dr G. D. Pitt for allowing us the use of the SERC high pressure facilities based at STL Harlow.

References

1. A. J. M. LICHNOWSKI and G. A. SAUNDERS, *J. Phys. C: Solid State Phys.* **9** (1976) 927.
2. *Idem, ibid.* **10** (1977) 3243.
3. J. M. N. van GOOR and H. M. G. J. TRUM, *J. Phys. Chem. Solids* **30** (1969) 1636.
4. Y. K. YOGURTCU. A. J. MILLER and G. A. SAUNDERS, *J. Phys. C: Solid State Phys.* **13** (1980) 685.
5. R. N. THURSTON and K. BRUGGER, *Phys. Rev.* **133** (1964) A1604.
6. R. N. THURSTON, *Proc. IEEE* **53** (1965) 1320.
7. R. W. KEYES, *IBM J. Res. Dev.* **5** (1961) 266.
8. *Idem, Solid State Phys.* **20** (1967) 37.
9. M. S. DRESSELHAUS, *J. Phys. Chem. Solids* **32** Suppl. 1 (1971) 3.
10. M. P. VECCHI and M. S. DRESSELHAUS, *Phys. Rev.* **B10** (1974) 771.
11. G. A. SAUNDERS and Y. K. YOGURTCU, *Phys. Lett.* **81A** (1981) 463.
12. K. BRUGGER, *Phys. Rev.* **137** (1965) A1826.
13. Tu HAILING and G. A. SAUNDERS, to be published.
14. N. G. PACE, G. A. SAUNDERS and Z. SÜMENGEN, *J. Phys. Chem. Solids* **31** (1970) 1467.
15. G. LIEBFRIED and W. LUDWIG, *Solid State Phys.* **12** (1961) 275.

Received 2 November
and accepted 20 December 1982